1. Zbigniew GORYCA[1], 2. Konrad DĄBAŁA[2], 3. Artur MORADEWICZ[3], 4. Maciej BOGUMIŁ[4], 5. Artur PAKOSZ[5]

Kielce University of Technology, Faculty of Environmental Engineering, Geomatics and Renewable Energy (1), Łukasiewicz Research Network – Institute of Electrical Engineering (2,3,4), Warsaw University of Technology, Institute of Automation and Robotics(5)
ORCID: 1.0000-0002-2015-7828; 2.0000-0002-0510-3784; 3.0000-0001-6092-5468; 4.0000-0002-5477-2394; 5.0000-0003-3059-0702

doi:10.15199/48.2024.01.16

Slow-speed motor for electric actuators

***Abstract**. The article presents a low-speed BLDC 180 W motor with a rotational speed of 470 rpm, and torque of about 3.7 Nm, designed for level crossing barrier drives. The parameters, calculations of electromagnetic fields and the results of laboratory tests of two motors with cores made of different types of sheet metal are presented.*

***Streszczenie.** W artykule przedstawiono dedykowany do napędów rogatkowych wolnoobrotowy silnik BLDC o mocy 180 W i prędkości obrotowej 470 1/min, dysponujący momentem około 3,7 Nm. Zaprezentowano parametry, obliczenia polowe obwodu elektromagnetycznego oraz wyniki badań laboratoryjnych dwóch wykonanych silników o rdzeniach wykonanych z różnych rodzajów blachy. (**Wolnoobrotowy silnik do siłowników elektrycznych**)*

Keywords: electric machines, electric actuators, BLDC motors, BLDC motor drive.
Słowa kluczowe: maszyny elektryczne, siłowniki elektryczne, silniki BLDC, napęd z silnikami BLDC.

Introduction

Electric actuators are a group of drives that has been developing very dynamically. They successfully compete with hydraulic actuators in the aviation and automotive industry, and are already widely used in the railway industry. Polish Railways operate several thousand railway crossings. Most of them are crossings with electric barriers closed for the duration of the train passage and with additional traffic lights. With the exception of hydraulic drives, all of them are driven by electric actuators. This applies to currently most popular crossing barrier drive of the EEG-3 type and the mechanical drive manufactured by Kombud Company. In both of them, a DC commutator motor drives the actuator lead screw through a belt drive, and the actuator causes the barrier to move. The main disadvantage of these solutions is high price of non-standard commutator motors and the need to periodically replace the brushes. In the case of a closed motor housing and lack of ventilation, dust from worn brushes settling inside the motor may short-circuit the commutator sections, which leads to failure. Therefore, it seems advisable to use BLDC motors (BrushLess Direct-Current motors) (without brushes and a mechanical commutator) in electric actuators. These motors do not require periodic check-ups, and their life cycle is limited only by the life cycle of the used bearings. An additional advantage of BLDC motors is the possibility of manufacturing them for an extremely low rotational speed, e.g., 470 rpm which eliminates the belt transmission in the level crossing barrier drive. The disadvantages of these motors include the need to use rotor position sensors [7, 8] (there are sensorless methods [6]) and the need to work with an electronic controller but the latter is compensated by the ease of speed control, which is useful when starting and stopping the level crossing barrier movement. Sensorless control methods are used in drive systems but with low starting torque, e.g. in pumps and fans, and in systems with low dynamics. For these reasons we developed, a low-speed 180 W BLDC motor with rotational speed of 470 1/min and torque of approximately 3.7 Nm, dedicated to crossing barrier drives. This motor can drive the lead screw without a gear in the Alstom's EEG3 drive or in a level crossing barrier drive manufactured by Kombud.

Design assumptions

The design of the motor was mainly guided by the closing and opening time requirements of the drive (15 s) and the mechanical torque required by the actuator. Motor power of 180 W, speed of 470 rpm and supply voltage of 24 VDC were assumed. These values were the input data for calculating the geometry of the magnetic circuit and motor winding. The excitation of the motor by N38 permanent magnets was also assumed. Due to the application and the short working time of the motor, the operating mode S2 5 min was assumed.

Motor design

The motor we developed is a typical brushless motor excited by permanent magnets located in the rotor. Most solutions use permanent magnets glued to the outer surface of the rotor [1, 2]. However, gluing magnets requires time and adherence to strict technological regimes (specific temperature and low air humidity) as well as special tools that base magnets during gluing. In addition, the magnets must be in the shape of segments of the ring, which involves a significantly increased price compared to rectangular magnets. Therefore, we decided to use cuboid magnets placed inside the rotor [2, 5]. Due to low rotational speed of the motor, the number of poles equal to 10 and the concentrated winding placed in the stator were chosen. In this case, the width of the yoke can be significantly reduced (which reduces the weight of the core) and the winding ends can be shortened (which reduces the weight of the copper used in the motor windings). Figures 1 and 2 show the shape of the stator and rotor sheets.

This design of the motor's magnetic circuit has several advantages: the magnets cannot detach from the rotor, as it can happen when they are glued on its surface, and they are less susceptible to demagnetization (they are placed inside the rotor). Also, fast and precise assembly is ensured - the magnets are inserted into the gaps. An additional advantage is the low price of typical, rectangular magnets. The disadvantage of the solution is that a part of the magnetic flux of each magnet is closed off by the lateral part of the magnetic circuit between the magnets. Therefore, the gaps should be as small as possible for technological reasons. In the developed motor, the rotor sheets were made by laser cutting and the side part of the magnetic socket was 0.8 mm wide. Thanks to this solution, the magnetic flux density in the motor gap was 0.6 T.

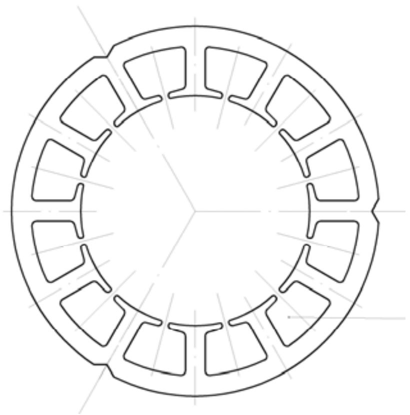

Fig. 1 Shape of the stator sheets of the developed motor

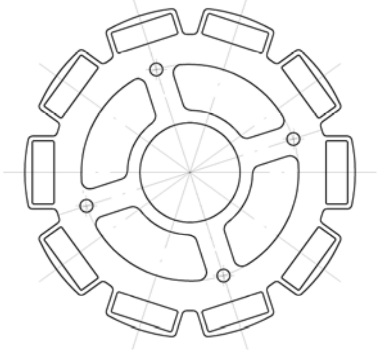

Fig. 2. Shape of the rotor sheets of the developed motor

Calculation of magnetic flux density in the components of magnetic circuit

The basis for calculating the dimensions of the magnets and the parameters of the winding are the electromagnetic calculations determining the induction in all components of the magnetic circuit for the assumed geometrical dimensions of the machine [3, 4, 9]. These calculations were carried out using the finite element method in the FEMM 4.2 program. The final calculation result for the selected rotor position is shown in Figure 3.

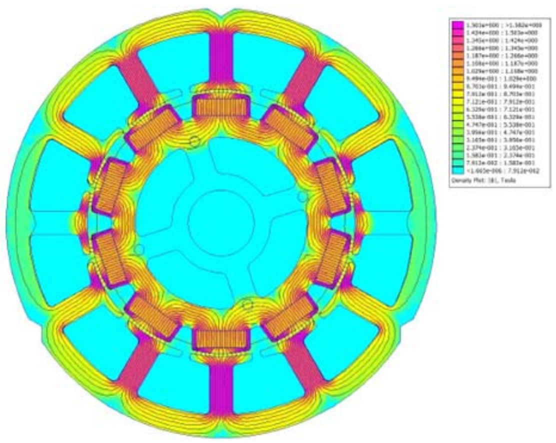

Fig. 3. Magnetic flux distribution in the magnetic circuit of the machine

As can be seen, the magnetic flux density value in any part of the magnetic circuit does not exceed 1.6 T. The calculations also show the possibility of reducing the width of the stator yoke and the possibility of increasing the area of the gaps reducing the mass of the rotor. For technological reasons (difficulties in core assembling when the yoke is too thin) we decided not to change these dimensions (the change is advisable in mass production). An important parameter of machines with permanent magnets is the value of the cogging torque affecting the vibrations and noise generated during the operation of the machine. In the case of the developed motor, of the length of 40 mm, the calculated cogging torque does not exceed 0.1 Nm.

Laboratory tests

Laboratory tests were carried out at the Research Laboratory of Electromobility and Intelligent Transport in the Łukasiewicz Research Network - Institute of Electrical Engineering in Warsaw. The tests included determination of basic motor parameters and measurements of winding and insulation resistance. Two motors with identical dimensions of the magnetic circuit and core length, but differing in winding parameters and magnetic material of the stator and rotor, were tested. In the first case, the magnetic circuit of the motor was made of a typical generator sheet of E530-50A-130 symbol and thickness of 0.5 mm. The magnetic circuit of the second motor was made of uninsulated and silicon-free sheet metal (sheet metal of DC01 symbol) and 1 mm thick. The basic design data of the motors are: torque 3.7 Nm at speed of 200 1/min, maximum speed 470 1/min and supply voltage 24 VDC. The test bench is shown in Fig. 4. A Yokogawa analyzer was used to determine the motor characteristics (electrical values and rotational speed were measured). An electronic scale was used to determine the power on the engine shaft. The torque was determined based on the pressure force of the dynamometer arm on the scale. The engine efficiency was determined using the direct method.

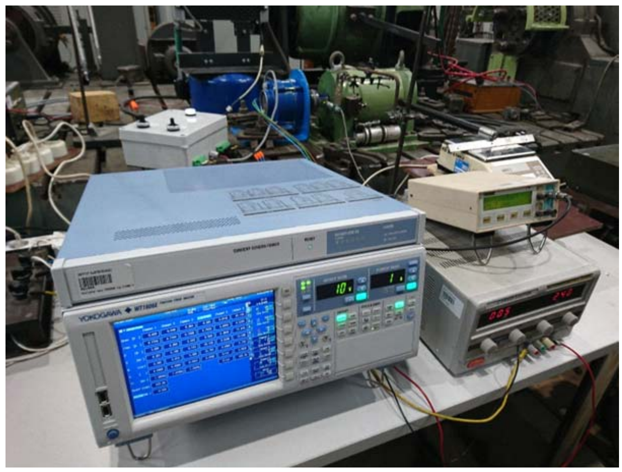

Fig 4. Test bench

The most important mechanical characteristics of the motors were determined (as presented below) and the cogging torque of both motors was measured (the average of measurements in ten rotor positions). In addition, in order to determine the efficiency, the voltage supplying the motor, the current consumed, the torque produced and the rotational speed were measured.

Characteristics $T(n)$ were made for the controller setting $n = n_{max}$ under varying load (fig. 5) and $T(n)$ and efficiency at constant torque (fig. 6);

T – shaft torque;

n – rotational speed;

n_{max} – maximal value of speed adjusted on controller.

In the characteristic shown in Figure 5, the drive system with a 1 mm motor does not maintain a constant torque, unlike the drive system with a 0.5 mm motor, which has a constant torque in the speed range of 90-350 rpm.

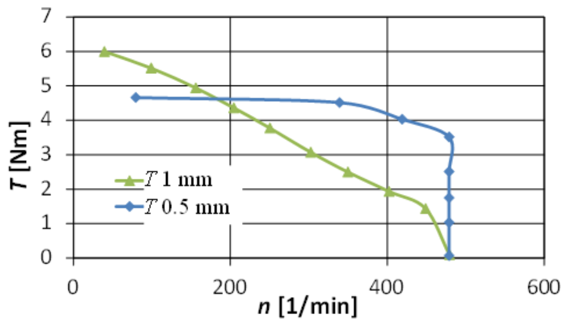

Fig. 5. Mechanical characteristics of the developed motors for the controller setting $n = n_{max}$

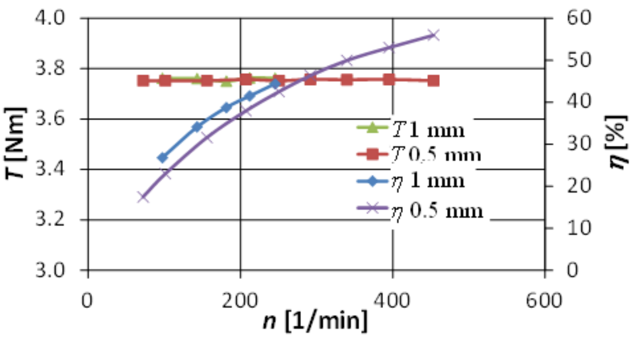

Fig. 6. Mechanical and efficiency characteristics of the developed motors at constant torque (T = const)

Figure 7 shows the characteristics of $T(n)$ for a controller setting of $n = 0.5n_{max}$ under varying load. In this case, the drive system maintains a constant set speed.

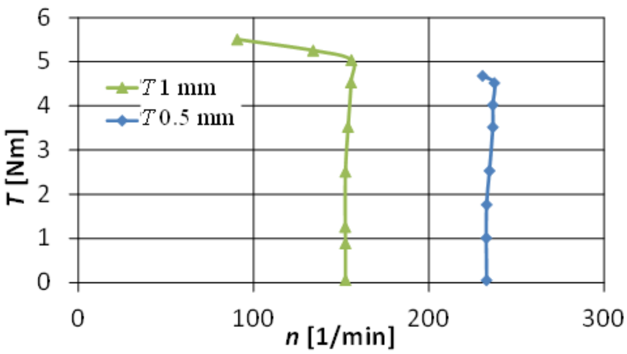

Fig. 7. Mechanical characteristics of the developed motors for the controller setting $n = 0{,}5n_{max}$

Figure 8 shows that the 1 mm motor achieves a higher torque (by approx. 66%) than the 0.5 mm motor.

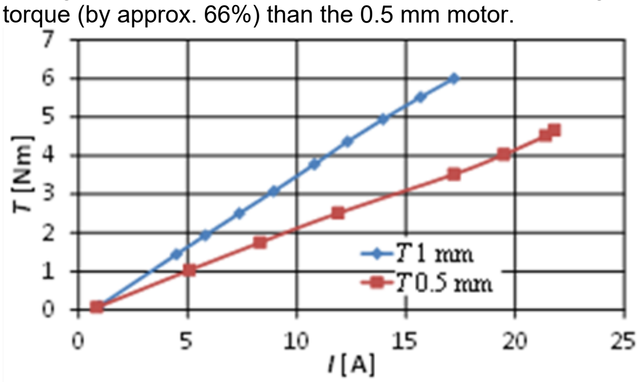

Fig. 8. Dependence of the generated torque on the current for the controller setting $n = n_{max}$

Table 1. The Temperature rise ($\Delta\vartheta$) of motor stator windings under different operating conditions (var – variable) for a test time of 5 min.

	$\Delta\vartheta$ [°C]	
	T=var	T=const n=var
1 mm, n_{max}	70	102
1 mm, $0{,}5n_{max}$	43	
0,5 mm, n_{max}	23	33
0,5 mm, $0{,}5n_{max}$	46	

Table 1 shows the temperature rise of the motor stator winding under different operating conditions for a test time of 5 min. The temperatures of the motor windings were measured using the resistive method after each characteristic was determined. The average temperature rise of the 1 mm motor winding is even more than 60° C higher, and for T = const even almost 70°C higher than that of the 0.5 mm motor. For the controller setting $n = n_{max}$, there is no significant difference in the temperature increase of the windings of both motors.

In order to verify the results of the cogging torque calculations, laboratory measurements of the cogging torque were carried out. Maximum cogging torque was measured using a balanced lever and precision weights. Ten measurements were made at different rotor positions and the arithmetic mean was calculated. The actual (maximum) value of the cogging torque is small for a multi-pole machine and amounts to 0.16 Nm. This is a large discrepancy in relation to the calculated value shown in Figure 9, but it should be noted that the results also include the friction torque of the motor bearings.

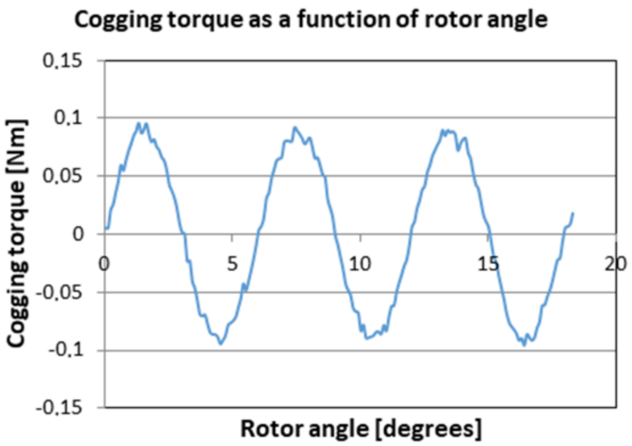

Fig. 9. Computed torque curve

Conclusions

As shown (Figure 7), at a setting of half the maximum speed, the motors can be loaded with a torque of 4.5 Nm. It should be emphasized that the motor parameters obtained are highly dependent on the controller used [10, 11]. The developed motors have low rotational speed and high torque and therefore can drive, without a gear, the lead screw of the actuator in level crossing barrier drives. This solution of the actuator simplifies its construction and facilitates the operation of the drives. In addition, the motor is cheaper than the existing geared motor and more available - domestic production. Due to short-term and occasional work, it can be worth considering whether the magnetic circuit of the motor should be made of high-loss sheet metal, because the energy consumption of crossing barrier drive is negligible. When using 1 mm thick sheets and their costly laser cutting, the price of the stator and rotor stacks is two times lower than the price of stacks made of generator sheet metal, which may be significant in mass production. The lower efficiency of the motor (within a certain speed range) is of secondary importance when used in a crossing barrier drive, because even on heavily trafficked railway lines, the drive operates for several minutes a day - one shift of the crossing barrier drive takes no more than 15 seconds.

***Authors**: dr hab. eng. Zbigniew Goryca, prof. PŚ, Kielce University of Technology, Faculty of Environmental Engineering, Geomatics and Renewable Energy, 25-314 Kielce, aleja Tysiąclecia Państwa Polskiego 7, E-mail: zgoryca@tu.kielce.pl; dr hab. eng. Konrad Dąbała, prof. IEl, Łukasiewicz Research Network – Institute of Electrical Engineering, 04-703 Warsaw, ul. Pożaryskiego 28, E-mail: konrad.dabala@iel.lukasiewicz.gov.pl; dr eng. Artur Moradewicz, Łukasiewicz Research Network – Institute of Electrical Engineering 04-703 Warszawa, ul. Pożaryskiego 28, E-mail: artur.moradewicz@iel.lukasiewicz.gov.pl; dr eng. Maciej Bogumił, Łukasiewicz Research Network – Institute of Electrical Engineering, ul. Pożaryskiego 28, E-mail: maciej.bogumil@iel.lukasiewicz.gov.pl; dr eng. Artur Pakosz, Warsaw University of Technology, Institute of Automation and Robotics, 00-661 Warszawa, plac Politechniki 1, E-mail: artur.pakosz@pw.edu.pl*

REFERENCES

[1] Dąbała K., Kaźmierkowski M., Converter-Fed Electric Vehicle (Car) Drives – A Critical Review, *Przegląd Elektrotechniczny*, nr 09 (2019), 1- 12
[2] Deepak M., Ranjeev A., Rajesh V., Sathiyaser A.: A Review of BLDC Motor: State of Art, *Advanced Control Techniques and Applications*,(2022), https://ieeexplore.ieee.org/stamp/stamp.jsp?arnumber=9774372
[3] Goryca Z., Różowicz S., Różowicz A., Pakosz A., Wachta H., Leśko M., Impact of Selected Methods of Cogging Torque Reduction in Multipolar Permanent-Magnet Machines, *Energies*, Vol. 13 (2022), Vol. 6108, 1-14
[4] Goryca Z., Ziółek M., Zależność momentu elektromagnetycznego silnika od geometrii obwodu magnetycznego, *Przegląd Elektrotechniczny*, nr 4 (2010), 217-219
[5] Goryca Z., A fan for solid-fuel furnaces, *Przegląd Elektrotechniczny*, nr 2 (2016), 129-131
[6] Goryca Z., Ziółek M., Metody bezczujnikowego sterowania silników BLDC, *Przegląd Elektrotechniczny*, nr 2 (2013), 128-132
[7] Kolano K., Stanowisko do analizy wpływu błędów rozmieszczenia czujników położenia wału silnika BLDC na jego pracę, *Przegląd Elektrotechniczny*, nr 8 (2016), 62-65
[8] Kolano K., Zastosowanie czujników fotooptycznych w torze pomiaru prędkości i położenia wirnika silnika BLDC, *Przegląd Elektrotechniczny*., nr 4 (2014), 169-172
[9] Chao Y. K-H., Chang L-Y., Hung C-Y., Design and Control of Brushless DC Motor Drives for Refrigerated Cabinets, *Energies* (2022), 15(9), 3453; https://doi.org/10.3390/en15093453
[10] Yang, Wang. X., Zhang R., Ding T., Tang R., The optimization of pole-arc coefficient to reduce cogging torque in surface-mounted permanent magnet motors, *IEEE Trans. Magn*., vol. 42, no. 4 (April 2006), 1135-1138
[11] Salah W.A., Ishak D., Hammadi K. J., Taib S., Development of a BLDC motor drive with improved output characteristics, *Przegląd Elektrotechniczny*, nr 3 (2011), 258-261